Coherent Terahertz Echo of Tunnel Ionization in Gases

N. Karpowicz and X.-C. Zhang*

Center for Terahertz Research, Department of Physics, Applied Physics and Astronomy, Rensselaer Polytechnic Institute, Troy, New York 12180, USA

(Received 13 October 2008; published 5 March 2009)

We study tunnel ionized electron wave packet dynamics during the initial transition from a gas to a plasma by detecting the terahertz radiation emitted in the process. Experimental and theoretical results show that much of the observed radiation is due to coherent buildup of bremsstrahlung released during the first electron-atom collision. Coherent control of the tunnel ionization process combined with *ab initio* modeling provides a real-time view of the initial stages of the formation of a laser-induced plasma and allows us to fully understand this important source of terahertz radiation.

DOI: 10.1103/PhysRevLett.102.093001 PACS numbers: 32.80.Fb, 32.80.Qk, 52.20.Fs, 52.25.Jm

The process of tunnel ionization [1–3] is at the heart of many important high intensity laser-matter interactions. The rapid, field-dependent creation of electron wave packets and their subsequent interaction with their parent atom and driving field permits us, among other things, to image atomic and molecular processes [4,5] and to generate coherent high-harmonic light [6,7]. Simultaneously, other work has used high intensity optical pulses to produce terahertz pulses in gases [8–15], which combine remarkably broad, continuous bandwidths [16–18] and high field strengths [19] in a source with exciting possibilities for remote sensing and the study of terahertz nonlinear interactions [20]. Since all of these effects are derived from the same physical process, the question arises as to how their products are complementary: What can be learned from one that is not visible in another? The interaction of electron wave packets with their source atoms and molecules and the development of detection and imaging technologies [21,22] have already provided new information about the internal electron and ion dynamics [4]. Now, using terahertz emission as a probe of the system, we observe the process turned outward, studying the wave packets propagating out into the surrounding gas and their first interaction with their neighbors. The experimental information gathered, coupled with computer modeling, gives us a new understanding of the transition from a gas to a plasma. Other fields of study, such as filament-induced breakdown spectroscopy [23], that utilize optically induced plasmas could benefit from our results.

In this Letter, we use terahertz waves generated in gases by the interaction of the atoms with optical fields composed of fundamental (800 nm) and second harmonic (400 nm) components. This effect was first reported by Cook and Hochstrasser [10] and treated through perturbation theory as a four-wave mixing process and later treated semiclassically by Kim *et al.* [13] and Thomson *et al.* [15], assigning the generation process to the formation of a current or polarization of the ionizing electrons, respectively. In the present work, we treat the ionization process quantum mechanically by numerically solving the time-dependent Schrödinger equation (TDSE) [24], which accurately describes the formation and acceleration of the relevant electron wave packets. Once formed, the wave packets freely propagate into the surrounding medium and eventually collide with a neighboring atom, losing coherence with the original laser-atom system. This process is illustrated in Fig. 1(a). The interaction emits terahertz radiation in two steps: first, terahertz photons are emitted due to the acceleration of the wave packets, which is given a net dipole moment through the asymmetry introduced by the two-color field. Next, when the wave packets collide with the neighboring atoms, they emit bremsstrahlung. Although the scattering time τ for each wave packet is random, the component of the velocity change along the direction of the laser polarization will be antiparallel to that of the wave packet propagation, resulting in coherent buildup of the resulting radiation at frequencies smaller than the mean of $\tau^{-1}/2$.

In order to calculate the creation of the wave packets and the corresponding terahertz radiation, the simulation is carried out in the velocity gauge [24] with the Hamiltonian (all equations are in atomic units) $H(t) = [\vec{p} + \vec{A}(t)]^2 + V(r)$.

The time-dependent laser vector potential $A(t)$ is linearly polarized and placed along the z axis of the coordinate system and describes the optical field

$$E(t) = E^o_\omega(t)\cos(\omega t) + E^o_{2\omega}(t + \phi/\omega)\cos(2\omega t + \phi), \quad (1)$$

where the functions $E(t)$ are 50 fs $\sin^2(t)$ pulse envelopes and ϕ is the relative delay between both the carrier and the envelope of the fundamental and second harmonic pulses. The simulations and experiments were carried out in argon since its electron spectrum can be treated accurately in the single active electron approximation [25,26]. At each step of the time propagation, the polarization of the system $P(t) = -\langle\Psi(t)|\hat{z}|\Psi(t)\rangle$ is taken, describing the first emission of terahertz radiation due to the asymmetric formation and acceleration of the wave packets in the bichromatic field. The grid radius is 1200 Bohr, large enough to contain nearly all of the electron probability density over the

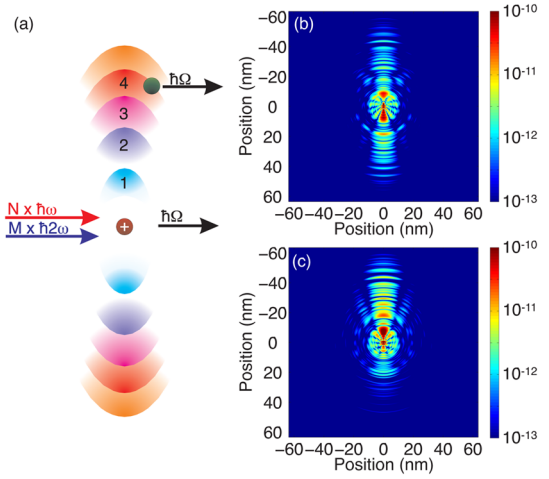

FIG. 1 (color online). (a) Illustration of the process by which the terahertz radiation is emitted. High intensity laser light composed of fundamental and second harmonic frequency components (ω and 2ω) interacts with the atom, resulting in tunnel ionization. Some of the wave packets formed in the ionization process are accelerated away from the atom, emitting terahertz radiation (Ω). They propagate away from the parent atom with quantized velocities, where the numbers indicate the number of energy quanta given to each wave packet. They then interact with their surroundings (in this case, a neutral atom) and emit bremsstrahlung, which adds coherently, resulting in a second source of terahertz radiation. (b),(c) Calculated electron density distributions for argon subjected to an intense optical field composed of fundamental and second harmonic pulses with phase differences of $5\pi/12$ and $11\pi/12$, resulting in minimal and maximal asymmetry, respectively. The ground state of the atom is removed, and a logarithmic scale (in atomic units) is utilized for clarity.

course of the optical pulse, which has a moderate peak electric field of 0.39 a.u. (2×10^{10} V/m) for the fundamental pulse and 0.039 a.u. for the second harmonic. Once the optical pulse is finished, the energy spectrum of the wave function is analyzed [27].

Changing the phase between the fundamental and second harmonic pulses results in a dramatic change in the angular distribution of the wave packets [28]. At this intensity, when the phase is near multiples of π, the distribution of the wave packets along the laser polarization axis is strongly asymmetric but almost symmetric near odd multiples of $\pi/2$. This is demonstrated in Figs. 1(b) and 1(c), where the probability densities for the phases corresponding to maximal and minimal terahertz generation are shown.

Once the laser-atom interaction is solved, the wave packet momenta can be used to describe the subsequent dynamics (the interaction with the surrounding gas) analytically by imposing an expanding disklike envelope on the wave packet. We will continue to observe the increasing polarization due to the propagation of the wave packets, but the amplitude n_i of each will be described by the differential equation

$$\frac{dn_i}{dt} = -\pi v_\perp v_\parallel r_A \rho t n_i, \tag{2}$$

where $v_\parallel$ is the wave packet velocity along the laser polarization axis (given by its central energy), $v_\perp$ describes its lateral spreading, r_A is the energy-dependent interaction radius [related to the total scattering cross section by $r_A = \sqrt{\sigma_{\mathrm{tot}}(E)/4\pi}$, for which values are well known [29]], and ρ is the number density of atoms or molecules. Because of the additional time dependence introduced by the influence of the dispersion of the wave packet on its scattering properties, the resulting time-dependent coherent polarization does not decay exponentially but rather takes the form

$$P_i(t) = -n_i^2(t)\langle z(t)\rangle = -n_i^2(0)e^{-at^2} v_\parallel t, \tag{3}$$

where $a = \pi r_A v_\parallel v_\perp \rho$ and $n_i(0)$ is the initial amplitude at a given electron energy. The total polarization is the sum of all individual wave packet polarization functions. In turn, the observed terahertz waveform, which is approximately proportional to the third time derivative of the polarization [30], will exhibit an oscillation due to the wave packets emitting bremsstrahlung at the stage in their evolution at which they lose coherence, marking the transition from states that could still be considered to be positive energy states of the laser-atom system to free electrons in a gas plasma.

To test these calculations, experiments were carried out with care taken to minimize the influence of macroscopic effects such as the focusing dynamics of high intensity pulses. The experiment is illustrated schematically in Fig. 2. The laser pulses were provided by a regenerative Ti:sapphire amplifier, with 1 kHz repetition rate, 720 μJ pulse energy, 800 nm central wavelength, and 80 fs pulse duration. The pump pulse was focused through a type-I β-barium borate (BBO) crystal to produce the second harmonic pulse. A 190 μm fused silica plate was placed in the beam path and could be rotated to change the relative phase between the two pulses (ϕ). The two pulses then

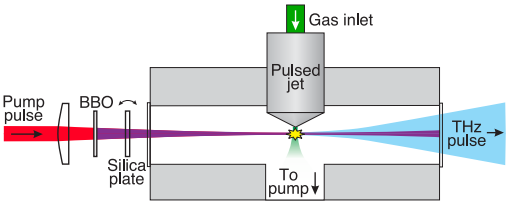

FIG. 2 (color online). Schematic diagram of the experimental setup. The amplified laser pulse is focused by a lens through a BBO crystal, generating a second harmonic pulse. The phase between the two pulses is adjusted using the fused silica plate. Synchronously with the laser pulses, gas pulses are produced in a gas jet inside of a vacuum chamber. When the gas and optical pulses intersect, the intense laser-gas interaction results in tunnel ionization and terahertz emission. The terahertz pulse exits the chamber through a Teflon window and is detected coherently via electro-optic sampling.

entered a small vacuum chamber containing a pulsed gas jet, which released 400 μs pulses of gas with a 500 μm diameter at a repetition rate of 100 Hz, synchronized with the laser repetition. The laser pulses interact with and ionize the gas pulse producing a terahertz pulse in the forward direction, which exits the chamber through a Teflon window. The terahertz pulse is collected and focused by a pair of off-axis parabolic mirrors and measured coherently in the time domain through electro-optic sampling in a 500 μm ZnTe crystal.

An essential factor in the tunnel ionization process for bichromatic light is the relative phase between the frequencies. In Fig. 3, we show the results of adjusting the phase, in calculation and experiment. In Figs. 3(a) and 3(b), the directional electron spectra are shown vs phase. Although the simulated second harmonic power is only 1% of the fundamental power, the change in directionality with phase is dramatic. Since the process can be coherently controlled, it has great potential for probing even more complicated systems. By combining the polarization from the TDSE calculations with the one subsequently derived from Eq. (3), we calculated the full time-dependent coherent polarization expected for each phase. The terahertz waveform can then be calculated by low-pass filtering of the third time derivative. This yields a set of waveforms corresponding to the phase-dependent terahertz emission from the two-step process. Excellent agreement between the form of the waveform calculated in this manner and the experimental observation is found as shown by overlapping the calculated waveforms over the measured ones in Fig. 3(c), confirming the validity of the simulation.

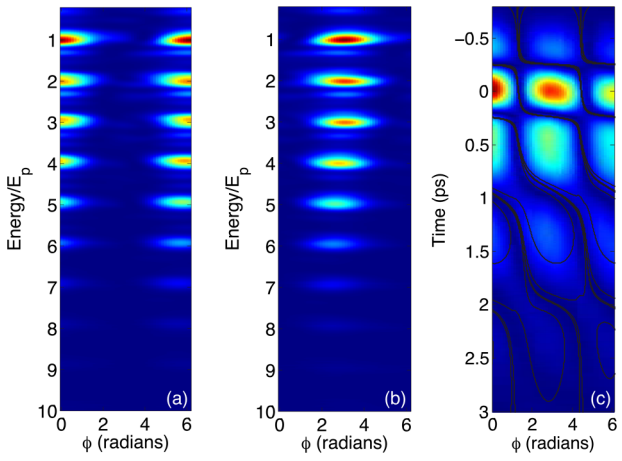

FIG. 3 (color online). Phase dependence of the process. (a), (b) Calculated electron spectra along the laser polarization axis ($\theta = 0$ and π, respectively), with energy in units normalized by the photon energy $E_p = 1.55$ eV. (c) Measured terahertz field amplitude at 50 torr backing pressure as a function of the phase ϕ, with superimposed contours taken from *ab initio* calculations of the waveforms made by combining the rising edge of the polarization from solving the TDSE and falling edge from Eq. (3).

By altering the backing pressure of the jet, we adjusted the atomic density at the focus [31], allowing for testing of Eq. (3). The focal atomic density ρ is estimated to be 6% of the reservoir density indicated by the backing pressure at room temperature. Figure 4 shows the results of changing the backing pressure of the jet. The series of waveforms in Fig. 4(a) shows that the amplitude and length of the oscillation due to scattering is modified with the density of the gas. As can be seen in Fig. 4(b), the pressure dependence mirrors the predictions of the wave packet model. As the pressure is lowered, the "echo" of the waveform is extended, indicating the increasing coherent lifetime of the wave packets. In Fig. 4(b), only the calculated bremsstrahlung contribution is shown, through the use of Eq. (3) and considering the modification of the waveform in the ZnTe crystal used for detection [32], giving an indication of the relative contribution of the second step of the emission process compared to the first. The waveforms were calculated with the assumption that the atomic population is dominated by neutral species since the ionization probability in the simulation was less than 1%; however, at higher intensities, scattering from ionized atoms will be dominant due to their larger cross sections.

The pressure-dependent extension in the time domain obviously translates into a redshift in the frequency domain, and thus the emission process exhibits a degree of

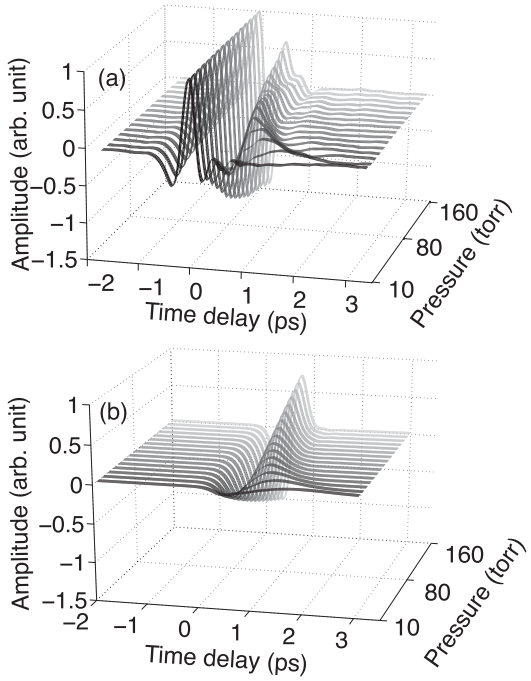

FIG. 4. Pressure dependence of the process. (a) Normalized waveform vs backing pressure (measured in the range from 10 to 160 torr in 10 torr steps). The echo portion visibly extends as the pressure is lowered, due to the increased coherence time of the electron wave packets in the medium. (b) Calculated contribution of coherent bremsstrahlung to the pulse for the same range of pressures using Eq. (3) and the electron spectrum calculated through solving the TDSE.

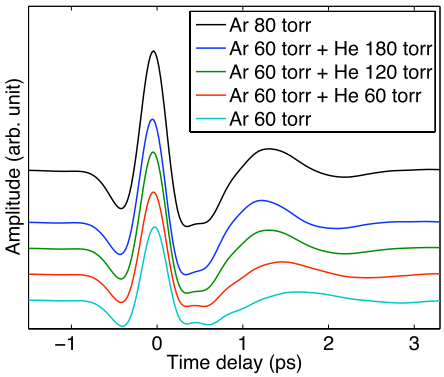

FIG. 5 (color online). Result of adding varying amounts of helium to the argon. Helium clearly changes the echo portion of the waveform, even though by itself it is not appreciably ionized by the laser pulse. The source of the modification is the coherent terahertz emission from an electron from an argon atom colliding with a helium atom. (Waveforms offset for clarity.)

pressure tunability, previously assigned to absorption of the terahertz radiation by free carriers [18]. Physically, this indicates that the wave packet loses coherence through a scattering process whose cross section is determined in part by the packet dimensions. To demonstrate that the effect was not due to free electron absorption (besides the very different functional form of the expected pulse), we added varying amounts of helium to the argon used for emission. For the intensities involved in this experiment, no measurable signal is observed from pure helium, since its ionization potential is too high for tunnel ionization to be appreciable. However, when argon is present, adding helium contracts the echo through its interaction with the external free electron wave packets, as shown in Fig. 5. Although helium cannot contribute to the first step in the generation process (ionization), it does participate in the second, causing the scattering process to occur more rapidly, culminating in a blueshift of the coherent bremsstrahlung. Adding helium results in an additional decay term in Eq. (2), such that

$$\frac{dn_i}{dt} = -\pi v_\perp v_\parallel r_{\mathrm{He}} \rho_{\mathrm{He}} t n_i - \pi v_\perp v_\parallel r_{\mathrm{Ar}} \rho_{\mathrm{Ar}} t n_i = -\pi v_\perp v_\parallel r_{\mathrm{mix}} \rho_{\mathrm{mix}} t n_i, \quad (4)$$

where r_{He} and r_{Ar} are the scattering radii of helium and argon, respectively, ρ_{He} and ρ_{Ar} are the respective number densities of the two gases, and $r_{\mathrm{mix}}\rho_{\mathrm{mix}} = r_{\mathrm{He}}\rho_{\mathrm{He}} + r_{\mathrm{Ar}}\rho_{\mathrm{Ar}}$. Therefore, adding additional helium effectively results in increasing the parameter a in Eq. (3), influencing the coherent polarization.

Observation of the emitted terahertz waves provides a unique look at the initial dynamics of a tunnel ionized gas as it turns into a plasma. By inducing an asymmetry through a second harmonic optical field, the electron wave packets formed can be used to probe the surrounding material through the terahertz radiation emitted by their interaction. In a gas, this information takes the form of the first scattering event with the surrounding material, marking the transition between atomic and plasma physics with an intense, coherent terahertz transient. The new understanding provided by this technique provides a way towards using the tunnel ionization process as a coherently controlled probe of the ion's environment and better manipulation of this useful source of terahertz pulses.

The authors thank Etienne Gagnon and Jianming Dai for useful discussions and acknowledge support from the Office of Naval Research and the National Science Foundation under Grant No. 0333314.

*zhangxc@rpi.edu

[1] L. V. Keldysh, Sov. Phys. JETP **20**, 1307 (1965).
[2] S. L. Chin, F. Yergeau, and P. Lavigne, J. Phys. B **18**, L213 (1985).
[3] M. Uiberacker *et al.*, Nature (London) **446**, 627 (2007).
[4] H. Niikura *et al.*, Nature (London) **417**, 917 (2002).
[5] M. Meckel *et al.*, Science **320**, 1478 (2008).
[6] P. B. Corkum, Phys. Rev. Lett. **71**, 1994 (1993).
[7] M. Hentschel *et al.*, Nature (London) **414**, 509 (2001).
[8] H. Hamster, A. Sullivan, S. Gordon, W. White, and R. W. Falcone, Phys. Rev. Lett. **71**, 2725 (1993).
[9] W. P. Leemans *et al.*, Phys. Plasmas **11**, 2899 (2004).
[10] D. J. Cook and R. M. Hochstrasser, Opt. Lett. **25**, 1210 (2000).
[11] M. Richter *et al.*, Phys. Rev. A **71**, 053819 (2005).
[12] M. Kreß *et al.*, Nature Phys. **2**, 327 (2006).
[13] K. Y. Kim, J. H. Glownia, A. J. Taylor, and G. Rodriguez, Opt. Express **15**, 4577 (2007).
[14] C. D'Amico *et al.*, Phys. Rev. Lett. **98**, 235002 (2007).
[15] M. D. Thomson, M. Kreß, T. Löffler, and H. G. Roskos, Laser Photon. Rev. **1**, 349 (2007).
[16] N. Karpowicz *et al.*, Appl. Phys. Lett. **92**, 011131 (2008).
[17] N. Karpowicz, J. Chen, T. Tongue, and X.-C. Zhang, Electron. Lett. **44**, 544 (2008).
[18] K. Y. Kim, A. J. Taylor, J. H. Glownia, and G. Rodriguez, Nat. Photon. **2**, 605 (2008).
[19] T. Bartel, P. Gaal, K. Reimann, M. Woerner, and T. Elsaesser, Opt. Lett. **30**, 2805 (2005).
[20] P. Gaal *et al.*, Nature (London) **450**, 1210 (2007).
[21] J. Ullrich *et al.*, J. Phys. B **30**, 2917 (1997).
[22] E. Gagnon *et al.*, Science **317**, 1374 (2007).
[23] J.-F. Daigle *et al.*, Opt. Commun. **278**, 147 (2007).
[24] H. G. Muller, Laser Phys. **9**, 138 (1999).
[25] M. J. Nandor, M. A. Walker, L. D. Van Woerkom, and H. G. Muller, Phys. Rev. A **60**, R1771 (1999).
[26] H. G. Muller, Phys. Rev. A **60**, 1341 (1999).
[27] K. J. Schafer and K. C. Kulander, Phys. Rev. A **42**, 5794 (1990).
[28] D. W. Schumacher and P. H. Bucksbaum, Phys. Rev. A **54**, 4271 (1996).
[29] S. Buckman and B. Lohmann, J. Phys. B **19**, 2547 (1986).
[30] T. Löffler *et al.*, Semicond. Sci. Technol. **20**, S134 (2005).
[31] D. M. Lubman, C. T. Rettner, and R. N. Zare, J. Phys. Chem. **86**, 1129 (1982).
[32] H. J. Bakker *et al.*, J. Opt. Soc. Am. B **15**, 1795 (1998).